Genome-Scale Methylation Analysis Identifies Immune Profiles and Age Acceleration Associations with Bladder Cancer Outcomes

Ji-Qing Chen[1], Lucas A. Salas[1], John K. Wiencke[2], Devin C. Koestler[3], Annette M. Molinaro[2], Angeline S. Andrew[4], John D. Seigne[5], Margaret R. Karagas[1], Karl T. Kelsey[6], and Brock C. Christensen[1,7]

ABSTRACT

Background: Immune profiles have been associated with bladder cancer outcomes and may have clinical applications for prognosis. However, associations of detailed immune cell subtypes with patient outcomes remain underexplored and may contribute crucial prognostic information for better managing bladder cancer recurrence and survival.

Methods: Bladder cancer case peripheral blood DNA methylation was measured using the Illumina HumanMethylationEPIC array. Extended cell-type deconvolution quantified 12 immune cell-type proportions, including memory, naïve T and B cells, and granulocyte subtypes. DNA methylation clocks determined biological age. Cox proportional hazards models tested associations of immune cell profiles and age acceleration with bladder cancer outcomes. The *partDSA* algorithm discriminated 10-year overall survival groups from clinical variables and immune cell profiles, and a semi-supervised recursively partitioned mixture model (*SS-RPMM*) with DNA methylation data was applied to identify a classifier for 10-year overall survival.

Results: Higher CD8T memory cell proportions were associated with better overall survival [HR = 0.95, 95% confidence interval (CI) = 0.93–0.98], while higher neutrophil-to-lymphocyte ratio (HR = 1.36, 95% CI = 1.23–1.50), CD8T naïve (HR = 1.21, 95% CI = 1.04–1.41), neutrophil (HR = 1.04, 95% CI = 1.03–1.06) proportions, and age acceleration (HR = 1.06, 95% CI = 1.03–1.08) were associated with worse overall survival in patient with bladder cancer. *partDSA* and *SS-RPMM* classified five groups of subjects with significant differences in overall survival.

Conclusions: We identified associations between immune cell subtypes and age acceleration with bladder cancer outcomes.

Impact: The findings of this study suggest that bladder cancer outcomes are associated with specific methylation-derived immune cell-type proportions and age acceleration, and these factors could be potential prognostic biomarkers.

Introduction

Bladder cancer is a malignant urogenital neoplasm and is classified into non–muscle-invasive bladder cancer (NMIBC) and muscle-invasive bladder cancer. In 2022, an estimated 81,000 new cases of bladder cancer and 17,000 deaths from the disease occurred in the United States (1). The common risk factors of bladder cancer are age, sex, and smoking. Bladder cancer is four times more common in men compared with women (2). About 90% of patients with bladder cancer are age 55 or older, and patients younger than 60 have a higher 10-year overall survival (OS) rate than patients older than 60 (3). Around 50% to 60% of new cases are attributed to smoking, and current smoking has a positive association with the risk of recurrence (4). The conventional treatment for bladder cancer is surgery or surgery in combination with chemotherapy drugs or intravesical immunotherapy [Bacillus Calmette-Guérin (BCG)] (5). Even though transurethral resection and immunotherapy generally control the disease (1, 6), the tumor recurrence rate is about 40% after treatment (7, 8). Predictive biomarkers that alert clinicians to recurrence would help to improve the clinical management of bladder cancer.

Circulating immune cell profiles have been associated with outcomes in patients with bladder cancer. For example, $CD8^+$ cell proportions were associated with a decreased risk of tumor recurrence (9). Also, an elevated neutrophil-to-lymphocyte ratio (NLR) has been associated with worse OS and higher recurrence rate (10, 11). Previously (12), we measured peripheral blood DNA methylation profiles of patients with NMIBC and applied cell-type deconvolution to estimate the proportions of six immune cell types (13). CD4T and CD8T cell proportions were associated with decreased risk of death and recurrence. Yet, there have been limited studies investigating the relationship of circulating immune profiles in bladder cancer with disease outcomes. Furthermore, subtypes of each major cell type have been shown to affect cancer development distinctly. For instance, cytotoxic $CD4^+$ T cells can kill the bladder tumor cells, and in contrast, regulatory $CD4^+$ T can suppress the activity of cytotoxic $CD4^+$ T cells and lead to tumor growth indirectly (14). To broaden the scope of the effects of circulating immune profiles on bladder cancer outcomes, it is necessary to investigate the association between leukocyte subtypes and bladder cancer outcomes.

[1]Department of Epidemiology, Geisel School of Medicine, Dartmouth College, Lebanon, New Hampshire. [2]Department of Neurological Surgery, University of California San Francisco, San Francisco, California. [3]Department of Biostatistics & Data Science, University of Kansas Medical Center, Kansas City, Kansas. [4]Department of Neurology, Geisel School of Medicine, Dartmouth College, Lebanon, New Hampshire. [5]Department of Surgery, Section of Urology, Geisel School of Medicine, Dartmouth College, Lebanon, New Hampshire. [6]Departments of Epidemiology and Pathology and Laboratory Medicine, Brown University, Providence, Rhode Island. [7]Departments of Molecular and Systems Biology, and Community and Family Medicine, Geisel School of Medicine, Dartmouth College, Lebanon, New Hampshire.

Corresponding Author: Brock C. Christensen, Geisel School of Medicine at Dartmouth College, Lebanon, NH 03756. E-mail: brock.christensen@dartmouth.edu

Cancer Epidemiol Biomarkers Prev 2023;32:1328–37

doi: 10.1158/1055-9965.EPI-23-0331

Recently, our group developed an enhanced method to perform high-resolution cell mixture deconvolution to resolve 12 immune cell types in blood using DNA methylation measures [naïve and memory B, CD4T, and CD8T, as well as regulatory T, monocyte, natural killer (NK) cells, neutrophils, basophils, and eosinophils; ref. 15]. Because DNA methylation involves gene regulation for cell lineage specification (16), cell-specific differentially methylated regions can be utilized to distinguish cell types with reference-based deconvolution (13, 17, 18). Also, DNA methylation cytometry is more efficient for immune profiling with high accuracy than flow cytometry and can be applied to archival specimens.

Epigenetic clocks have been developed to estimate chronologic age or physiologic age in regard to aging outcomes, such as cancers and all-cause mortality (19–21). Age acceleration derived from these clocks has been associated with prospective risk in lung, kidney, and pancreatic cancer (22–24). Moreover, age acceleration has been associated with outcomes in other cancers (25, 26). Though only a few studies have reported the association of age acceleration with bladder cancer risk, they have not exhibited consistent results nor mentioned the subtype of bladder cancer they investigated. For example, one study showed that Pheno and Grim age acceleration were positively associated with the prospective risk in bladder cancers (22). Another study reported that Horvath and Hannum age acceleration was not associated with bladder cancer risk (27). Because aging is one of risks of bladder cancer (28), we investigated the association of age acceleration with bladder cancer outcomes.

Here, we hypothesized that DNA methylation-derived immune cell proportions and age acceleration are associated with bladder cancer outcomes. We applied our new methylation cytometry approach for extended immune cell resolution to DNA methylation profiles of archival blood samples from a population-based study containing NMIBC ($N = 601$) patients. We then tested the association of cancer outcomes with each leukocyte subtype proportion and age acceleration. We also used *partDSA* (29), a classification and regression trees method, and a semi-supervised recursively partitioned mixture model (*SS-RPMM*; ref. 30), to group/cluster our subjects based on cancer outcomes, patients' demographics, tumor characteristics, and methylation profiles of specific CpG loci.

Materials and Methods

Study subjects and samples

A detailed description of subjects who participated in the current study is available in prior studies (31–33). Briefly, bladder cancer subjects were recruited from three phases of a New Hampshire population-based case–control study (34). The first phase collected blood samples from 331 individuals diagnosed between July 1994 and June 1998 (phase I). The second phase collected blood samples from 243 individuals diagnosed between July 1998 and December 2001 (phase II). The third study phase collected blood samples from 194 individuals diagnosed between July 2002 and December 2004 (phase III). Patients with bladder cancer were identified using the New Hampshire State Cancer Registry and hospital cancer registry (patients in phase III were identified using the hospital cancer registry only). Patients' OS data were from the National Death Index, and tumor recurrence data were ascertained through chart review. We performed four comprehensive National Death Index (NDI) searches for the years 2008, 2010, 2014, and 2018 to identify cases of death. In addition, the New Hampshire State Cancer Registry had previously reported some deaths to us through their conducted searches. During each NDI search, we included all bladder cancer case–control study participants who had not been previously matched with an NDI death. To ensure accurate matching, we followed the NDI-recommended method and utilized the code and algorithms provided by the NDI to score the matches. Furthermore, we applied the NDI score interpretation using the recommended NPCR algorithm (35) to enhance the accuracy of our findings. Subjects without histopathology re-review, muscle-invasive status, tumor grade, or smoking status were excluded from the study. The remaining 601 patients with NMIBC were used in downstream statistical analyses. In addition, 40 patients received BCG in phase I, 30 received BCG in phase II, and 19 received BCG in phase III. All patients with BCG treatment had their blood drawn after BCG treatment, and all blood samples were taken after the initial diagnosis. This study was approved by the Dartmouth Human Research Protection Program (Institutional Review Board; approval number STUDY00010107). The written informed consent was obtained from the patients and the studies were conducted in accordance with Belmont Report.

DNA extraction, qualification, and bisulfite modification

After the blood draw, blood samples were kept at 4°C and frozen within 24 hours. DNA was extracted from blood samples using the QIAamp DNA Blood Kit (Qiagen) according to the manufacturer's protocol. Extracted DNA quantity and quality were assessed with Qubit 3.0 Fluorometer (Life Technologies) and Fragment Analyzer (Advanced Analytical). Then, extracted DNA underwent bisulfite conversion using EZ DNA Methylation Kit (Zymo Research) according to the manufacturer's protocol. Approximately 750 ng of bisulfite-modified DNA was used as input for the DNA methylation array.

DNA methylation profiling

After DNA extraction, quantification, and bisulfite modification, Infinium MethylationEPIC Bead Chips (Illumina, Inc.) were used to measure the DNA methylation status of bisulfite-modified DNA samples. Raw probe intensity data, iDAT files, from the methylation array were processed through *preprocessNoob* using *minfi* (RRID: SCR_012830; ref. 36), and quality control was performed using *ENmix* (37) R package. To distinguish from background noise, samples with more than 5% of probes with a detection $P > 1.0 \times 10^{-6}$ were not included. In addition, we dropped 32,713 probes that were not detected in more than 10% of the samples. Then, the bias of type-2 probe values was corrected using *BMIQ* (RRID:SCR_003446; ref. 38) from *watermelon* (RRID:SCR_001296; ref. 39) R package, and the *ComBat* (RRID: SCR_010974; ref. 40) was used to adjust for batch effects. Next, 106,522 probes previously reported to be cross-reactive, SNP-associated, non-CpG (CpH) methylation, and sex-specific were excluded (41). After these exclusions, 726,856 CpGs remained for downstream statistical analysis. The annotation for CpG sites was from *IlluminaHumanMethylationEPICanno.ilm10b4.hg19*.

Statistical analysis

Methylation age was estimated with the function *methyAge* from the *ENmix* (37) R package implementation of the methylation age estimation. Age acceleration was defined as the residual from a regression of methylation age on chronologic age. Cell-type proportions were estimated with the *projectCellType_CP* from the *FlowSorted.Blood.EPIC* (RRID:SCR_022540; ref. 13) R package. The NLR was calculated according to the ratio of neutrophil proportion to lymphocyte proportion.

Ten-year OS was defined as the time interval from the date of initial diagnosis to death. Patients alive or lost to follow-up were censored at the last follow-up. Similarly, 10-year recurrence-free survival (RFS)

was defined as the time interval from the date of initial diagnosis to the first tumor recurrence or death, whichever occurred first, and patients alive and without tumor recurrence or lost to follow-up were censored at the last follow-up. For OS and RFS, survival times were truncated at 10 years. In univariate and multivariable analyses, *coxph* from the *survival* (RRID:SCR_021137) R package was used to fit Cox proportional hazards models to evaluate the association between bladder cancer outcomes and each variable. Only immune cell profiles significantly associated with bladder cancer outcomes in the univariate Cox model were subjected to multivariable analyses. *Cox.zph* from the *survival* R package was employed to test the proportional hazards assumption. Predictors with assumption violations were included as strata in the Cox models. The linearity assumption was examined with the *ggcoxfunctional* from the *survminer* (RRID:SCR_021094) R package. We conducted 2% winsorization on immune cell profiles identified to violate the linearity assumption. FDR-corrected P value of < 0.05 was the significance threshold on multivariable analysis.

To explore interactions between clinical variables and immune cell proportions in survival analysis, we applied a partitioning deletion/substitution/addition algorithm [*partDSA* (29, 42); R package] for model building employing the inverse probability censoring weighted-L2 loss function. Those variables (age, Hannum or Pheno age acceleration, sex, tumor grade, smoking status, BCG treatment status, and immune cell type proportions) associated with 10-year OS were included in the multivariable model as input. The *partDSA* approach resulted in three groups of subjects that were based on neutrophil and CD8 naïve cell proportions. After the model was built, corresponding Kaplan–Meier curves were generated, and HRs and 95% confidence intervals (CI) were calculated using the Cox model.

To identify a novel set of blood DNA methylation profiles associated with cancer outcomes, we applied a *SS-RPMM* algorithm (30). This method uses the recursive partitioning mixture model (*RPMM*), demonstrating an effective and efficient unsupervised clustering procedure for methylation data (43–46). To avoid overfitting and provide for validation of the model, we randomly split the total population into a training and testing set at a 2:1 ratio, stratified by deceased status (whether subjects were deceased or censored within 10 years) to balance the distribution of outcome status between sets. We used the 10% most variable CpG loci in methylation beta values across all samples. After splitting subjects and subsetting CpGs, a series of Cox proportional hazards models were fit using the training set for each selected CpG loci adjusted for age, age acceleration, sex, tumor grade, smoking status, BCG treatment status, and immune cell-type proportions associated with 10-year OS of patients with NMIBC. Next, Cox-scores ($|\beta|/se(\beta)$, where $\beta =$ the proportional hazards estimate of the log-HR, and $se =$ the standard error) were computed for each of the selected CpG loci, and Cpg loci were ranked based on the Cox scores. Subsequently, the top M (range: 5–50) loci with the largest absolute Cox scores were chosen using a x-fold cross-validation *RPMM* with the smallest median P value of the log-rank test for each potentially optimal number (M) of CpG loci in the training set. Then, *RPMM* was fit to the testing set for clustering subjects using the optimal M-selected CpG loci with the largest absolute Cox score, predicting the methylation class membership for the subjects. Then, all patients with NMIBC were clustered using *RPMM* based on the methylation levels of the optimal CpG sites. Finally, we evaluated the association of *RPMM* class membership with OS using Cox proportional hazards models.

Data availability

All datasets generated and analyzed during this current study are available in the Gene Expression Omnibus repository at GSE183920.

Results

Characteristics of subjects

DNA methylation profiles were obtained from 601 peripheral blood samples from patients with NMIBC using the Human MethylationEPIC array. The study group was 455 (75.7%) men, 306 (50.9%) former-smokers, 192 (32.0%) current-smokers, 89 (14.8%) with BCG treatment, and had a median age of 66 (**Table 1**). The distribution of chronologic age, methylation age, and age acceleration is shown in Supplementary Fig. S1A. Cell-type proportions were estimated for each patient using methylation cytometry (Supplementary Fig. S1B). Stratifying on median time from diagnosis to blood draw, patient and tumor characteristic summary statistics showed similar distributions. Furthermore, we observed no significant associations of immune profile variables with time from diagnosis to blood draw. To assess the potential modification of results by time to the blood draw, we performed an analysis testing the relation of immune profile variables with patient outcome, stratifying patients into two groups based on median time to the blood draw. We did not observe differences between associations of immune variables with outcomes between the groups based on time to blood draw.

Risk of bladder cancer outcomes

First, we examined associations of three major methylation age clocks, Horvath age (19), Hannum age (21), and DNAmPhenoAge (20),

Table 1. Characteristics of subjects.

	NMIBC ($n = 601$)
Age	
Median (IQR)	66 (57–71)
Pheno age acceleration	
Median (IQR)	−0.41 (−4.28 to 3.65)
Hannum age acceleration	
Median (IQR)	−0.10 (−2.53 to 2.54)
Sex	
Male	455 (75.7%)
Female	146 (24.3%)
Tumor grade	
Low grade	450 (74.9%)
High grade	151 (25.1%)
Smoking status	
Never	103 (17.1%)
Former	306 (50.9%)
Current	192 (32.0%)
BCG: Immunotherapy	
No	512 (85.2%)
Yes	89 (14.8%)
Time from diagnosis to blood draw (days)[a]	
Median (IQR)	319 (176–569)
NLR	
Median (IQR)	1.96 (1.38–2.86)
10-year survival status	
Alive	413 (68.7%)
Deceased	178 (29.6%)
Censored	10 (1.7%)
10-year recurrence-free status[b]	
Alive and no tumor recurrence	224 (37.3%)
Tumor recurrence or deceased	371 (61.7%)
Censored	6 (1.0%)

[a]All blood samples were taken after the diagnosis.
[b]Whether patient with tumor recurrence or deceased within 10 years.

Table 2. Cox proportional hazards multivariable models for demographic and tumor characteristics of 601 patients with NMIBC (for Pheno age acceleration).

	10-year overall survival HR (95% CI)	10-year recurrence-free survival[a] HR (95% CI)
Age	1.08 (1.06–1.10)	1.02 (1.01–1.03)
Pheno age acceleration	1.06 (1.03–1.08)	1.02 (1.00–1.03)
Sex		
Male		
Female	0.50 (0.33–0.78)	
Tumor grade		
Low grade		
High grade	1.58 (1.15–2.17)	1.49 (1.18–1.88)
Smoking status		
Non-smoker		
Former-smoker	1.35 (0.82–2.22)	1.56 (1.13–2.15)
Current-smoker	1.87 (1.10–3.16)	1.69 (1.20–2.38)
BCG treatment		
No		
Yes	0.89 (0.58–1.34)	

Abbreviations: CI, confidence interval; HR, hazard ratio; NMIBC, non–muscle-invasive bladder cancer.
[a]Stratification was used on sex and BCG treatment status for proportional assumption.

with bladder cancer outcomes. Our findings showed that Horvath age acceleration was not associated with 10-year OS (Supplementary Table S1). Because the Horvath clock was developed using data from a subset of CpG loci on the Illumina HumanMethylation27 (27K) CpG BeadChip (~27,000 features) compared with the Hannum and PhenoAge clocks (which were developed using 20 times more features with data from CpGs on the Illumina HumanMethylation450 (450K) and EPIC (850K) BeadChips), we focused on Hannum and Pheno age acceleration in subsequent analyses. Then, we fit multivariable Cox proportional hazards models for demographic and tumor characteristic variables to investigate associations with 10-year OS and RFS. For patients with NMIBC, age, age acceleration, smoking, and high tumor grade were associated with worse RFS and OS. Women had a better survival outcome compared with men (**Table 2**; Supplementary Table S2).

Next, the association between immune cell-type proportions and bladder cancer patient outcomes was investigated. We fit multivariable Cox models for immune cell-type proportions associated with bladder cancer outcomes in Cox univariate models (**Table 3**; Supplementary Table S3). CD4T memory, CD8T memory, and NK cell proportions were associated with a decreased risk of death. Whereas NLR, CD8T naïve, and neutrophil cell proportions were each associated with an increased risk of death. In analyses of RFS, CD4T memory was associated with a decreased risk of tumor recurrence, and NLR, monocyte, and regulatory T cell proportions were associated with an increased risk of tumor recurrence (**Table 3**; Supplementary Table S3). Hazard estimates for associations of demographic and tumor characteristic variables with outcomes were similar after adjusting for cell composition. Because there was a stronger (smaller *P* value) association of immune cell profiles with 10-year OS compared with 10-year RFS, subsequent analyses are focused on 10-year OS of patients with NMIBC. Because BCG treatment may affect immune cell composition, we performed a sensitivity analysis limiting our analysis to patients not receiving BCG treatment and observed results consistent with those obtained for all patients with NMIBC (**Table 3**; Supplementary Table S4).

Clinical and immune profiles recursive partitioning analysis

To partition the covariate space and explore interactions of clinical variables with immune cell proportions in 10-year OS, we applied a partitioning deletion/substitution/addition [*partDSA* (29)] algorithm for model building (**Fig. 1A**). *partDSA* is an analytic algorithm employing recursive partitioning. It uses loss functions to build clinically interpretable predictors of risk for a given event based on the covariate information. In brief, this method divides the covariate space into mutually exclusive regions and stratifies patients into distinct risk groups with respect to an outcome. As a result, it can make guidelines for estimating a patient's prognosis from clinical and biological information (42). Age, Hannum or Pheno age acceleration,

Table 3. Cox proportional hazards models of immune cell proportions and NMIBC patient outcomes (for Pheno age acceleration).

	10-year overall survival			10-year recurrence-free survival		
	Univariate model	Multivariable[a] model		Univariate model	Multivariable[b] model	
	HR (95% CI)	HR (95% CI)	FDR	HR (95% CI)	HR (95% CI)	FDR
NLR	1.49 (1.37–1.62)	1.36 (1.23–1.50)	6.9×10^{-9}	1.14 (1.06–1.22)	1.10 (1.01–1.18)	0.046
Memory B cell	0.82 (0.72–0.94)	0.89 (0.78–1.02)	0.13	0.94 (0.87–1.03)		
Naïve B cell	0.86 (0.79–0.94)	0.93 (0.86–1.00)	0.09	0.99 (0.94–1.04)		
Memory CD4T cell	0.92 (0.90–0.95)	0.95 (0.93–0.98)	3.8×10^{-3}	0.97 (0.96–0.99)	0.98 (0.96–0.99)	0.046
Naïve CD4T cell	0.87 (0.82–0.93)	0.98 (0.92–1.04)	0.48	0.95 (0.92–0.99)	0.99 (0.95–1.02)	0.46
Memory CD8T cell	0.96 (0.94–0.99)	0.95 (0.93–0.98)	3.8×10^{-3}	0.99 (0.97–1.01)		
Naïve CD8T cell	0.84 (0.73–0.96)	1.21 (1.04–1.41)	0.03	0.93 (0.86–1.02)		
Monocyte	1.06 (1.02–1.11)	1.01 (0.96–1.06)	0.74	1.05 (1.02–1.08)	1.03 (1.00–1.07)	0.07
Neutrophil	1.06 (1.05–1.08)	1.04 (1.03–1.06)	2.0×10^{-6}	1.01 (1.00–1.02)	1.01 (0.99–1.02)	0.31
Regulatory T cell	1.27 (1.08–1.49)	1.16 (0.98–1.36)	0.12	1.20 (1.06–1.35)	1.17 (1.03–1.32)	0.046
NK cell	0.92 (0.87–0.98)	0.92 (0.86–0.98)	0.03	0.98 (0.94–1.02)		
Basophil	1.51 (1.24–1.85)	1.26 (1.01–1.56)	0.07	1.16 (0.99–1.35)		
Eosinophil	1.02 (0.95–1.10)			1.03 (0.98–1.08)		

Note: Winsorization was used on the top 2% or the last 2% (only Neu) values for fitting linearity assumption.
Abbreviations: CI, confidence interval; HR, hazard ratio; NLR, neutrophil to lymphocyte ratio; NMIBC, non-muscle-invasive bladder cancer.
[a]The model controlling for age, sex, tumor grade, smoking status, BCG treatment status, and Pheno age acceleration.
[b]The model controlling for age, stratified sex, tumor grade, smoking status, stratified BCG treatment status, and Pheno age acceleration.

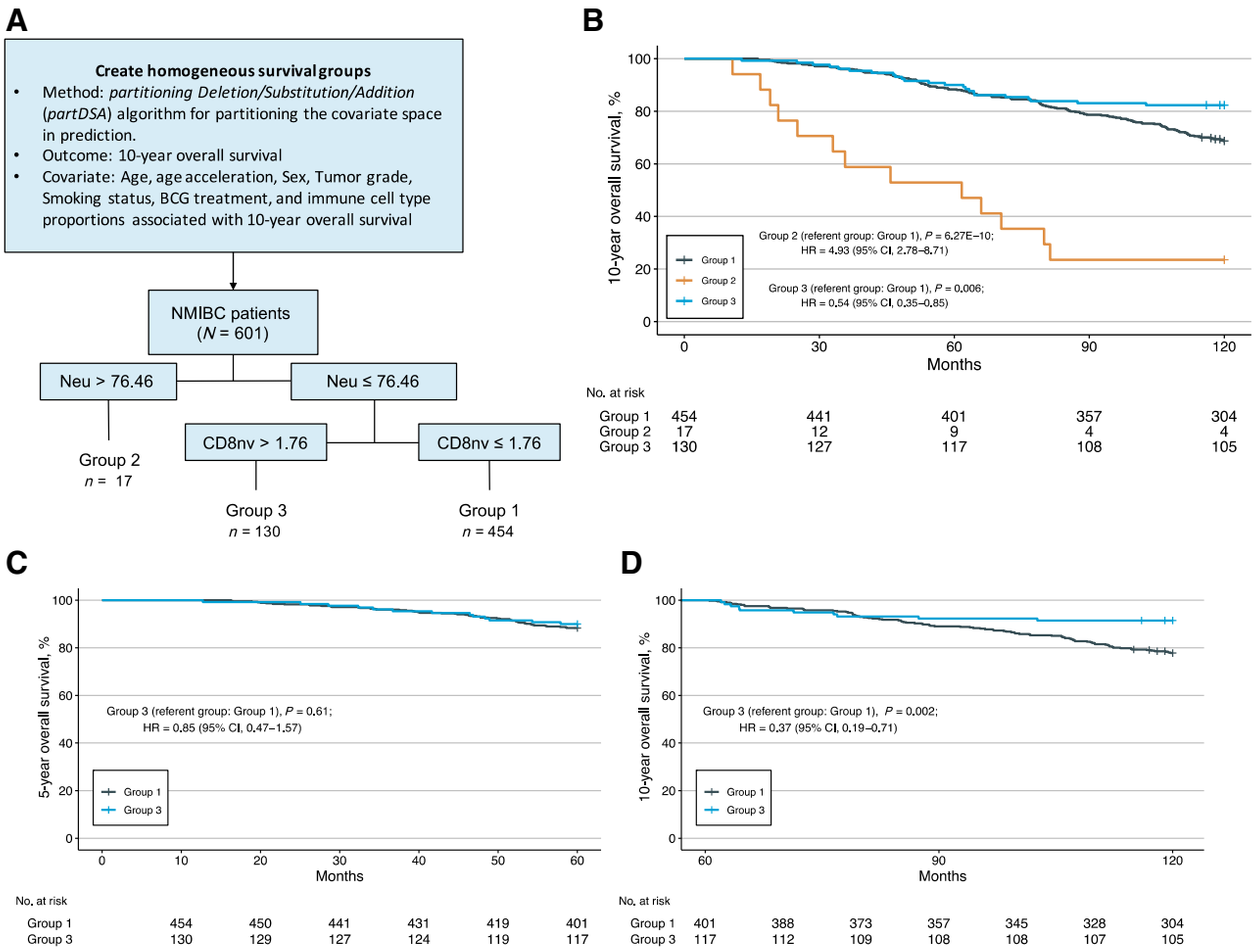

Figure 1.

Clinical and immune profiles recursive partitioning analysis, and 10-year OS Kaplan–Meier curves stratified by the grouping result from *partDSA* in patients with NMIBC: **A,** *partDSA* model setting and analysis results. For 601 patients with NMIBC, the neutrophil cell proportion in peripheral blood was the primary node, with the CD8 naïve cell proportion as the secondary node. Patients with NMIBC fell into one of three risk groups. Group 1 consisted of the 454 patients who had neutrophil cell proportions ≤76.46 and CD8 naïve cell proportions ≤1.76. Group 2 consisted of the 17 patients who had neutrophil cell proportions >76.46. Group 3 consisted of the 130 patients who had neutrophil cell proportions ≤76.46 and CD8 naïve cell proportions >1.76. CD4T memory, CD8T naïve, CD8T memory, NK cells, and neutrophils cell proportions were employed in the model using Pheno age acceleration; B memory, CD4T memory, CD8T naïve, CD8T memory, regulatory T, NK cells, neutrophils, and basophils cell proportions were employed in the model using Hannum age acceleration. Both models generated the same partitioning results. **B,** Kaplan–Meier curves are shown based on clinical and immune profiles recursive partitioning analysis. **C,** 5-year OS Kaplan–Meier curves in patients with NMIBC in Groups 1 and 3. **D,** Five- to 10-year OS Kaplan–Meier curves in patients with NMIBC in Groups 1 and 3 who were deceased or censored after 60 months. *P* values for log-rank tests are shown. All Kaplan–Meier curves are univariate analyses without adjusting for other variables. CI, confidence intervals; HR, hazard ratio; Neu, neutrophil.

sex, tumor grade, smoking status, BCG treatment status, and immune cell type proportions associated with 10-year OS were included in the model as input. The outcome was 10-year OS. The *partDSA* analysis divided subjects into three groups based on neutrophil and CD8 naïve cell proportions. The patients with NMIBC with neutrophil proportion >76.46 had the worst 10-year OS (Group 2, $n = 17$, HR = 4.93, 95% CI = 2.78–8.71) compared with Group 1 patients (patients with neutrophil cell proportions ≤76.46 and CD8 naïve cell proportions ≤1.76; $n = 454$; **Fig. 1B**). Although the 10- and 5-year OS rates (**Fig. 1C**) for Groups 1 and 3 were not statistically significantly different, we observed that their corresponding Kaplan–Meier curves separated after 5 years. To further investigate the difference between 10-year OS in Group 1 and Group 3, we selected the patients with NMIBC in Groups 1 and 3 whose time intervals from the date of initial diagnosis to death or the last follow-up were greater than 5 years (sample size: Group 1 = 401; Group 3 = 117), using the Kaplan–Meier method to observe 10-year OS. As we expected, for patients with time intervals from the date of initial diagnosis to death or last follow-up of more than 5 years, Group 3 patients (neutrophil proportion ≤76.46, CD8T naïve proportion >1.76) had better 10-year OS (HR = 0.37, 95% CI = 0.19–0.71) compared with Group 1 patients (**Fig. 1D**). Next, we examined the distribution of immune cell-type proportions, methylation age, and age acceleration in the three groups. Among the groups, patients with NMIBC in Group 2 had lower B naïve, eosinophil, monocyte, NK, CD4T memory, CD4T naïve, CD8T memory, and CD8T naïve proportions compared with other groups. Also, patients

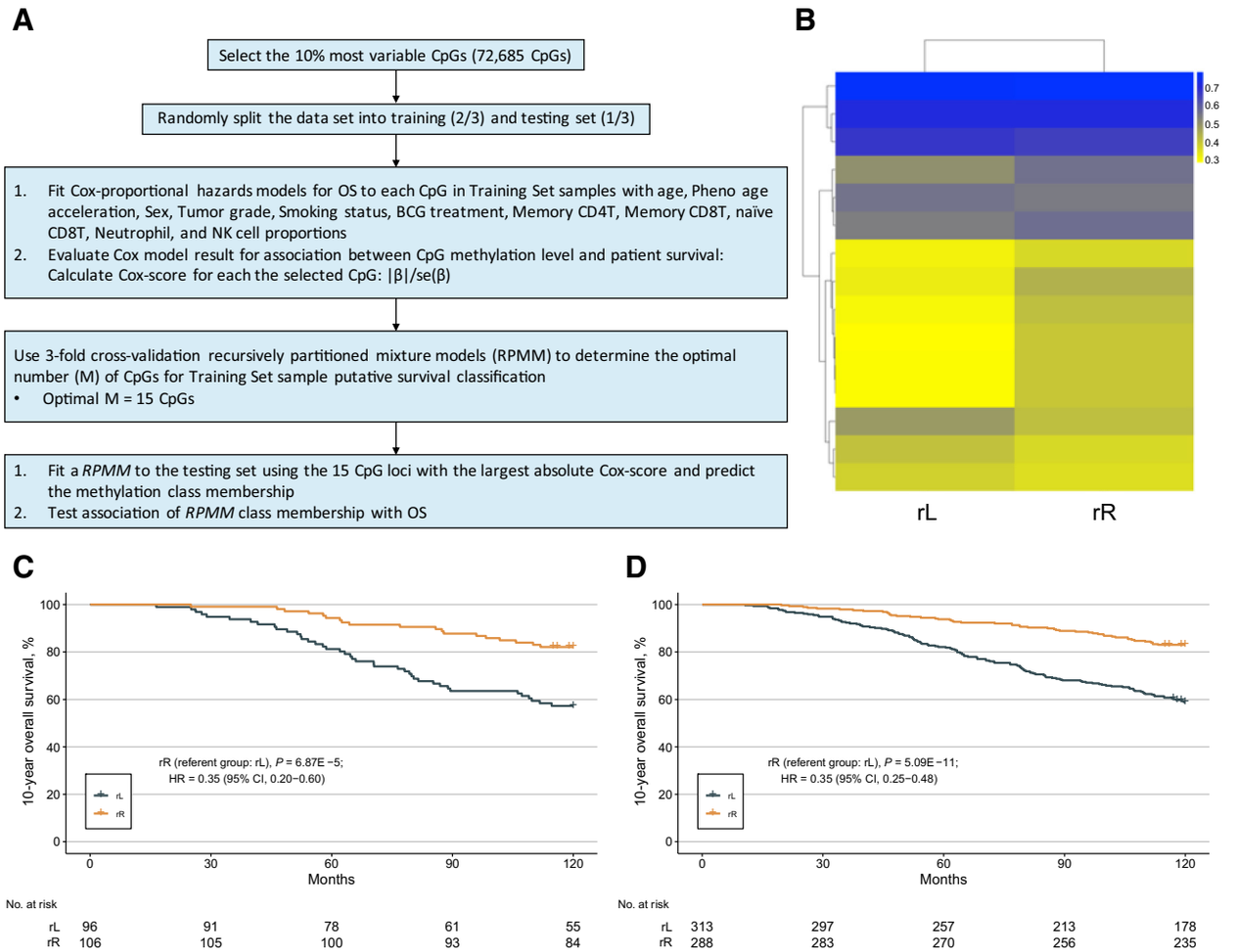

Figure 2.

SS-RPMM for 10-year OS in patients with NMIBC (for Pheno age acceleration): **A,** Data analysis schematic of *SS-RPMM* used for identification of blood DNA methylation profiles associated with NMIBC. **B,** Heat map of predicted class memberships for the observations in all patients with NMIBC using the average beta values of the 15 CpG loci with the largest absolute Cox scores. **C,** Kaplan–Meier curves of 10-year OS stratified by the *SS-RPMM* classification of 202 patients with NMIBC in the testing set by the 15 CpG loci. **D,** Kaplan–Meier analysis of 10-year OS. Ten-year OS curves stratified by the grouping result from *SS-RPMM* in all patients with NMIBC. *P* values for log-rank tests are shown. All Kaplan–Meier curves are univariate analyses without adjusting for other variables; CI, confidence intervals; HR, hazard ratio; *SS-RPMM*, semi-supervised recursively partitioned mixture model.

in Group 2 had higher neutrophil proportion, NLR, chronologic age, methylation age, and age acceleration compared with other groups (Supplementary Fig. S2).

SS-RPMM for 10-year OS

To investigate whether we could identify a blood DNA methylation profile associated with NMIBC survival, we applied a *SS-RPMM* method. The workflow is illustrated in **Fig. 2A** and Supplementary Fig. S3A. The subjects in the testing set were assigned to cluster membership using the methylation profiles of the optimal CpG sites [Supplementary Table S5A (Pheno) and Supplementary Table S5B (Hannum)]. Then, all patients with NMIBC were clustered using *RPMM* based on the methylation levels of the optimal CpG sites, resulting in two classes, rR and rL ["R" and "L" corresponded with branches in the dendrogram; r stands for root; **Fig. 2B** (Pheno); Supplementary Fig. S3B (Hannum)]. Methylation class membership was significantly associated with 10-year OS; patients in cluster rR had a more favorable 10-year OS compared with those in cluster rL in both the testing set [HR = 0.35, 95% CI = 0.20–0.60; **Fig. 2C** (Pheno); HR = 0.38, 95% CI = 0.21–0.68; Supplementary Fig. S3C (Hannum)] and when using all patients with NMIBC [HR = 0.35, 95% CI = 0.25–0.48; **Fig. 2D** (Pheno); HR = 0.37, 95% CI = 0.27–0.52; Supplementary Fig. S3D (Hannum)]. Then, we compared the distribution of immune cell-type proportions, chronologic age, methylation age, and age acceleration. Consistent with the models in **Table 3** and Supplementary Table S3, we observed that patients in cluster rR (n = 288) had significantly higher B memory, B naïve, CD4T memory, CD4T naïve, CD8T memory, and NK cell proportions and had significantly lower basophil, eosinophil, monocyte, neutrophil cell proportions, NLR, chronologic age, methylation age, and age acceleration compared with patients in cluster rL (n = 313; Supplementary Fig. S4A and S4B). The model using Hannum age acceleration had similar results shown in Supplementary Fig. S4C and S4D.

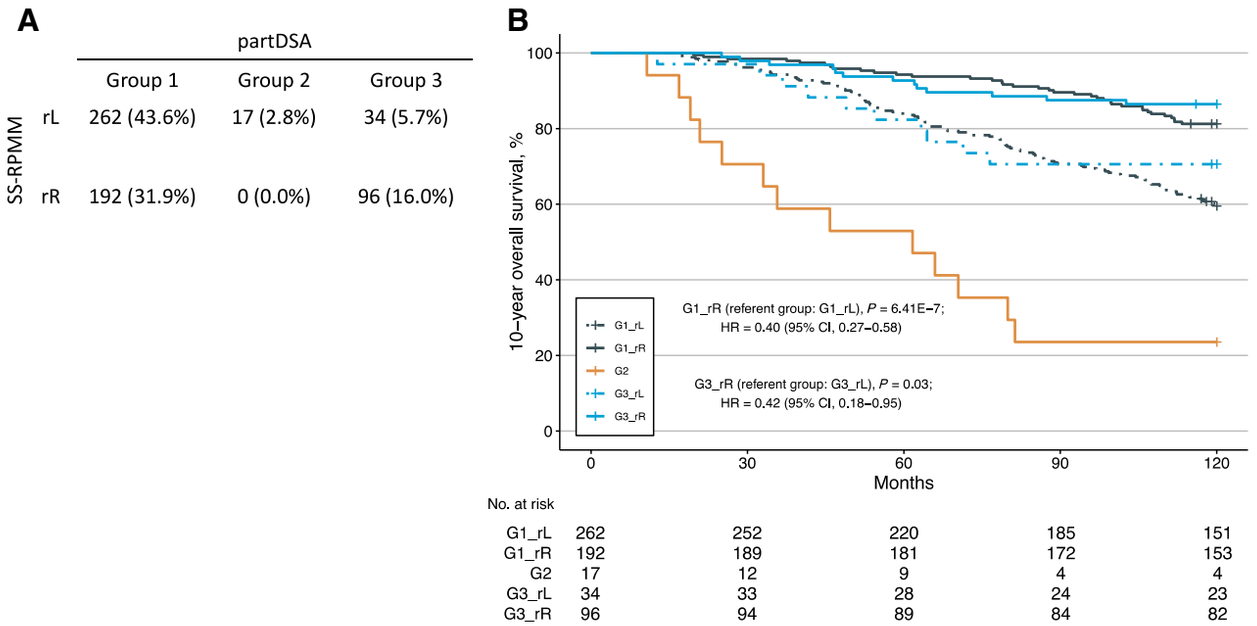

Figure 3.

Kaplan–Meier analysis of 10-year OS based on the grouping results from both *partDSA* and *SS-RPMM* in all patients with NMIBC (for Pheno age acceleration): **A,** contingency table based on the grouping results from both *partDSA* and *SS-RPMM* in all patients with NMIBC. **B,** Ten-year OS curves of all five groups. *P* values for log-rank tests are shown. All Kaplan–Meier curves are univariate analyses without adjusting for other variables. CI, confidence intervals; HR, hazard ratio; NMIBC, non-muscle-invasive bladder cancer; *partDSA*, partitioning deletion/substitution/addition algorithm; *SS-RPMM*, semi-supervised recursively partitioned mixture model.

Combined results from immune cell proportions and methylation profile groups

The two methods above used immune profiles (*partDSA*) and DNA methylation profiles (*SS-RPMM*) to explore the association of these profiles with OS, respectively. We were curious whether we could combine immune and methylation information to produce a guideline for estimating a patient's prognosis. To gain a deeper understanding of interactions between clinical variables, immune cell proportions, and blood DNA methylation profiles in 10-year OS, we allocated patients with NMIBC based on clustering results from *partDSA* and *SS-RPMM* analyses in five groups (Supplementary Table S6). Groups 1 and 3, from the *partDSA* analysis, were divided into two subgroups based on the *SS-RPMM* analysis (**Fig. 3A**; Supplementary Fig. S5A). In Kaplan–Meier analysis, patients in Group 2 still had the worst 10-year OS rate among all groups. Within the Group 1 patients, the group G1_rR had better 10-year OS than the group G1_rL [HR = 0.40, 95% CI = 0.27–0.58; **Fig. 3B** (Pheno); HR = 0.45, 95% CI = 0.31–0.65; Supplementary Fig. S5B (Hannum)]. Consistent with Group 1 patients, in Group 3 patients, the group G3_rR had better 10-year OS compared with the group G3_rL [HR = 0.42, 95% CI = 0.18–0.95; **Fig. 3B** (Pheno); HR = 0.35, 95% CI = 0.15–0.79; Supplementary Fig. S5B (Hannum)].

Discussion

This study aimed to test the relation of bladder cancer outcomes with high-resolution immune profiles using methylation cytometry and cell-independent methylation states in blood. In prior work, we observed that CD4T and CD8T proportions were associated with the decreased risk of death and tumor recurrence in patients with NMIBC (12); however, the results were not generalizable to naïve and memory subtypes of CD4T and CD8T cells. With recent advances in methylation cytometry for immune profiling (15), we were able to examine the association between the proportions of regulatory T cells, eosinophils, basophils, naïve and memory subtypes of CD4T, CD8T, and B cell and bladder cancer outcomes. Consistent with our previous study, NLR was associated with an increased risk of death and tumor recurrence in patients with NMIBC. For CD4T and CD8T cell subsets, CD4T memory and CD8T memory cell proportions were associated with a decreased risk of death. However, only CD4T memory cell proportion was associated with a reduced risk of death and tumor recurrence. One possible explanation for the different observations is that we introduced age acceleration into the models. This might confound the association between CD8T cell proportions subtypes and bladder cancer outcomes. Here, we identified associations between immune cell subtypes and age acceleration with bladder cancer outcomes. These factors could be potentially prognostic biomarkers of bladder cancer.

Few studies have shown age acceleration from multiple age clocks to be associated with bladder cancer outcomes, and even then, they do not show consistent results (22, 27). In our study, the direction of hazard estimates among cell type proportions was similar. However, outcome associations with immune profile differed in Cox multivariable models controlling for Pheno and Hannum age acceleration. The observed difference was potentially due to the training methods of clocks. Unlike Hannum age using chronologic age as a surrogate, Pheno age mainly focuses on aging outcomes, such as cancers, diet, and all-cause mortality, hence, Pheno age can capture age-related outcomes and perform well in predicting survival compared with chronologic methylation clocks, such as Hannum and Horvath clocks. Horvath age acceleration was not associated with bladder cancer outcomes. One potential explanation is that the Horvath clock was built mainly using a subset of CpGs on the 27K methylation array platform, which had approximately 20 times fewer CpGs than the 450K and EPIC array platforms used for the developing of the Hannum and PhenoAge

clocks. Furthermore, various cell and tissue types were used to develop the Horvath clock. However, Hannum and PhenoAge clocks were built based on data from blood DNA measures.

Our findings suggest that elevated NLR, neutrophil, basophil, regulatory T, and decreased CD4T memory cell proportions increased the risk of death and tumor recurrence in patients with bladder cancer. These findings met our expectations, consistent with previous studies demonstrating that peripheral blood NLR levels were associated with an increased risk of NMIBC recurrence after surgery (47–49). Moreover, basophil count was significantly associated with an increased risk of recurrence in patients with BCG-treated bladder cancer (50). One study indicated that peripheral (neutrophil × platelet)/(lymphocyte) was inversely correlated with a high risk of tumor recurrence in NMIBC (51). Even though some peripheral immune profiles we found had not been revealed to be associated with bladder cancer outcomes, these immune profiles in the tumor microenvironment had been reported to be associated with bladder cancer outcomes. For instance, higher regulatory T cell infiltration in the tumor microenvironment was associated with a shorter RFS (52), and regulatory T cell frequency within the tumor was inversely correlated with RFS in patients with NMIBC (53). Future work that integrates the assessment of cell-type proportions in the tumor microenvironment and periphery associated with bladder cancer outcomes would be of value.

The optimal 15 CpG loci selected by *SS-RPMM* using the model adjusting for Pheno age acceleration, and the optimal 50 CpG loci selected by *SS-RPMM* using the model adjusting for Hannum age acceleration track to several genes that have been reported to be involved in bladder cancer development. Sprouty-related EVH1 domain-containing protein 2 (*SPRED2*), is a negative regulator of the *ERK-MAPK* pathway, and has been reported to have increased mRNA and protein expression in NMIBC compared with carcinoma *in situ* and infiltrating urothelial carcinoma (54). In addition, patients with higher *SPRED2* mRNA levels had better OS compared with low expression group (54). Peroxisome proliferator-activated receptor gamma (*PPARG*) high-activation has been reported to promote cell-cycle G_2 arrest and apoptosis, leading to suppression of tumor growth and better prognosis in patients with bladder cancer (55). Fibrous sheath interacting protein 1 (*FSIP1*) was overexpressed in protein and mRNA levels of bladder tumor tissues and cancer cell lines (56, 57). Besides, *FSIP1* overexpression was associated with worse outcomes (56). Phosphorylated MAPK 14 (*MAPK14*) was overexpressed in bladder cancer cell lines and tissues (58). Furthermore, phosphorylated *MAPK14* could combine and regulate *RUNX2*, which was identified in our previous study through epigenome-wide association study (12), to promote the proliferation and migration of bladder cancer (58). Consistent with our findings, patients with a worse survival rate (rL group) had lower methylation levels in the CpG site, cg16145324, located in the *MAPK14* gene region (Supplementary Table S5B).

To further investigate the interactions between clinical variables, immune profiles, and DNA methylation levels, we performed both *partDSA* and *SS-RPMM*. Though patients with NMIBC were divided into three groups using *partDSA*, the Kaplan–Meier curves for Group 1 and 3 patients were not significantly different. Interestingly, when we applied the optimal CpG loci selected by *SS-RPMM*, patients in Groups 1 and 3 were grouped into two groups, with a significant difference in 10-year OS. This finding illustrated the importance of methylation levels of specific CpG sites in evaluating bladder cancer prognosis.

While this study carefully evaluated the association of cancer outcomes with peripheral immune cell type proportions, there were potential study limitations. For instance, BCG treatment has been reported to affect immune cell composition (50, 51, 59) and methylation profiles (60). We do not have detailed information, such as cycle numbers or responsiveness for each patient, though only a few patients (14.8%) in our study received BCG treatment. In addition, our sensitivity analysis that limited to patients who did not receive BCG treatment demonstrated consistent results with the overall NMIBC group. In addition, case ascertainment for our population-based study resulted in a median time from diagnosis to study blood draw is 319 days in our dataset. Furthermore, some confounding factors, such as obesity (61), alcohol consumption (62), and type 2 diabetes (63), have been reported to affect peripheral immune cell distribution. However, we had incomplete information on these potential covariates.

Taken together, our analysis applied the latest differentially methylated region library and highlighted several peripheral immune profiles that were associated with bladder cancer outcomes. We assessed interactions between clinical variables, immune cell proportions, and blood DNA methylation profiles in 10-year OS using *partDSA* and *SS-RPMM* analyses, clustering patients with NMIBC into five groups according to the methylation levels of the optimal CpG loci, neutrophil, and CD8T naïve cell proportions. While few studies have investigated the association between bladder cancer outcomes and peripheral immune profiles, our findings provide insight into the potential of peripheral immune profiles to serve as prognostic biomarkers in bladder cancer. Future work examining immune profiles in tumor tissues as well as DNA methylation profiles of patients with bladder cancer is needed to integrate interactions between bladder cancer outcomes, methylation levels, peripheral immune environment, and tumor microenvironments to further validate the feasibility of methylation-derived immune profiles for epigenetic biomarkers of bladder cancer.

Authors' Disclosures

L.A. Salas reports grants from CDMRP/Department of Defense (W81XWH-20-1-0778) and NIGMS (P20 GM104416) during the conduct of the study; in addition, has a patent for U.S. Provisional Patent Application Enhanced DNA Methylation Library for Deconvoluting Peripheral Blood (63/148,695) pending. J.D. Seigne reports grants from NIH and CDMRP/Department of Defense during the conduct of the study; other support from Johnson & Johnson outside the submitted work. K.T. Kelsey reports other support from Cellintec outside the submitted work; in addition, has a patent 10,619,211 issued. B.C. Christensen reports grants from NIH during the conduct of the study; personal fees from University of California San Fransico outside the submitted work; in addition, has a patent for Enhanced DNA Methylation Library for Deconvoluting Peripheral Blood pending. No disclosures were reported by the other authors.

Disclaimer

The funders had no role in study design, data collection, data analysis, or data interpretation.

Authors' Contributions

J.-Q. Chen: Conceptualization, formal analysis, validation, investigation, visualization, methodology, writing–original draft, writing–review and editing. **L.A. Salas:** Conceptualization, formal analysis, supervision, investigation, methodology, writing–review and editing. **J.K. Wiencke:** Conceptualization, methodology, writing–review and editing. **D.C. Koestler:** Conceptualization, methodology, writing–review and editing. **A.M. Molinaro:** Conceptualization, methodology, writing–review and editing. **A.S. Andrew:** Data curation. **J.D. Seigne:** Data curation. **M.R. Karagas:** Conceptualization, methodology, writing–review and editing. **K.T. Kelsey:** Conceptualization, methodology, writing–review and editing. **B.C. Christensen:** Conceptualization, resources, formal analysis, supervision, funding acquisition, validation, methodology, project administration, writing–review and editing.

Acknowledgments

B.C. Christensen is supported by the NIH grant numbers R01CA216265. B.C. Christensen, M.R. Karagas, and L.A. Salas are supported by the NIH grant number P20GM104416. M.R. Karagas is supported by the NIH grant number R01CA057494. B.C. Christensen and K.T. Kelsey are supported by the NIH grant number R01CA253976. L.A. Salas is supported by the CDMRP/Department of Defense W81XWH-20-1-0778. J.K. Wiencke and A.M. Molinaro are supported by the NIH grant number P50CA097257. J.K. Wiencke is supported by the Robert Magnin Newman Endowed Chair in Neuro-oncology and the NIH grant numbers R01CA207360. D.C. Koestler is supported by the NCI Cancer Center Support Grant P30 CA168524 and the Kansas Institute for Precision Medicine COBRE (supported by the National Institute of General Medical Science award P20 GM130423).

The publication costs of this article were defrayed in part by the payment of publication fees. Therefore, and solely to indicate this fact, this article is hereby marked "advertisement" in accordance with 18 USC section 1734.

Note

Supplementary data for this article are available at Cancer Epidemiology, Biomarkers & Prevention Online (http://cebp.aacrjournals.org/).

Received April 3, 2023; revised June 6, 2023; accepted July 28, 2023; published first August 1, 2023.

References

1. Siegel RL, Miller KD, Fuchs HE, Jemal A. Cancer statistics, 2022. CA Cancer J Clin 2022;72:7–33.
2. Saginala K, Barsouk A, Aluru JS, Rawla P, Padala SA, Barsouk A. Epidemiology of bladder cancer. Med Sci 2020;8:15.
3. Lin W, Pan X, Zhang C, Ye B, Song J. Impact of age at diagnosis of bladder cancer on survival: a surveillance, epidemiology, and end results-based study 2004–2015. Cancer Control 2023;30:10732748231152322.
4. Hou L, Hong X, Dai M, Chen P, Zhao H, Wei Q, et al. Association of smoking status with prognosis in bladder cancer: a meta-analysis. Oncotarget 2017;8:1278–89.
5. DeGeorge KC, Holt HR, Hodges SC. Bladder cancer: diagnosis and treatment. Am Fam Physician 2017;96:507–14.
6. Antoni S, Ferlay J, Soerjomataram I, Znaor A, Jemal A, Bray F. Bladder cancer incidence and mortality: a global overview and recent trends. Eur Urol 2017;71:96–108.
7. Witjes JA. Management of BCG failures in superficial bladder cancer: a review. Eur Urol 2006;49:790–7.
8. Soukup V, C?apoun O, Cohen D, Hernández V, Babjuk M, Burger M, et al. Prognostic performance and reproducibility of the 1973 and 2004/2016 world health organization grading classification systems in non–muscle-invasive bladder cancer: a European association of urology non-muscle invasive bladder cancer guidelines panel syst. Eur Urol 2017;72:801–13.
9. Lin CT, Tung CL, Tsai YS, Shen CH, Jou YC, Yu MT, et al. Prognostic relevance of preoperative circulating CD8-positive lymphocytes in the urinary bladder recurrence of urothelial carcinoma. Urol Oncol 2012;30:680–7.
10. Tan YG, Eu E, Lau Kam On W, Huang HH. Pretreatment neutrophil-to-lymphocyte ratio predicts worse survival outcomes and advanced tumor staging in patients undergoing radical cystectomy for bladder cancer. Asian J Urol 2017;4:239–46.
11. Kang M, Jeong CW, Kwak C, Kim HH, Ku JH. Preoperative neutrophil-lymphocyte ratio can significantly predict mortality outcomes in patients with non-muscle invasive bladder cancer undergoing transurethral resection of bladder tumor. Oncotarget 2017;8:12891–901.
12. Chen JQ, Salas LA, Wiencke JK, Koestler DC, Molinaro AM, Andrew AS, et al. Immune profiles and DNA methylation alterations related with non-muscle-invasive bladder cancer outcomes. Clin Epigenetics 2022;14:14.
13. Salas LA, Koestler DC, Butler RA, Hansen HM, Wiencke JK, Kelsey KT, et al. An optimized library for reference-based deconvolution of whole-blood biospecimens assayed using the Illumina HumanMethylationEPIC BeadArray. Genome Biol 2018;19:64.
14. Oh DY, Kwek SS, Raju SS, Li T, McCarthy E, Chow E, et al. Intratumoral CD4+ T cells mediate anti-tumor cytotoxicity in human bladder cancer. Cell 2020;181:1612–25.
15. Salas LA, Zhang Z, Koestler DC, Butler RA, Hansen HM, Molinaro AM, et al. Enhanced cell deconvolution of peripheral blood using DNA methylation for high-resolution immune profiling. Nat Commun 2022;13:761.
16. Suelves M, Carrió E, Núñez-Álvarez Y, Peinado MA. DNA methylation dynamics in cellular commitment and differentiation. Brief Funct Genomics 2016;15:443–53.
17. Reinius LE, Acevedo N, Joerink M, Pershagen G, Dahlén SE, Greco D, et al. Differential DNA methylation in purified human blood cells: implications for cell lineage and studies on disease susceptibility. PLoS One 2012;7:e41361.
18. Houseman EA, Accomando WP, Koestler DC, Christensen BC, Marsit CJ, Nelson HH, et al. DNA methylation arrays as surrogate measures of cell mixture distribution. BMC Bioinformatics 2012;13:86.
19. Horvath S. DNA methylation age of human tissues and cell types. Genome Biol 2015;16:R115.
20. Levine M, Lu A, Quach A, Chen B, Assimes T, Bandinelli S, et al. An epigenetic biomarker of aging for lifespan and healthspan. Aging 2018;10:573–91.
21. Hannum G Guinney J Zhao L Zhang L Hughes G Sadda SV, et al. Genome-wide methylation profiles reveal quantitative views of human aging rates. Mol Cell 2013;49:359–67.
22. Dugue PA, Bassett JK, Wong EM, Joo JHE, Li S, Yu C, et al. Biological aging measures based on blood DNA methylation and risk of cancer: a prospective study. JNCI Cancer Spectr 2021;5:pkaa109.
23. Levine ME, Hosgood HD, Chen B, Absher D, Assimes T, Horvath S. DNA methylation age of blood predicts future onset of lung cancer in the women's health initiative. Aging 2015;7:690–700.
24. Chung M, Ruan M, Zhao N, Koestler DC, De Vivo I, Kelsey KT, et al. DNA methylation ageing clocks and pancreatic cancer risk: pooled analysis of three prospective nested case-control studies. Epigenetics 2021;16:1306–16.
25. Xiao C, Miller AH, Peng G, Levine ME, Conneely KN, Zhao H, et al. Association of epigenetic age acceleration with risk factors, survival, and quality of life in patients with head and neck cancer. Int J Radiat Oncol Biol Phys 2021;111:157–67.
26. Xiao C, Beitler JJ, Peng G, Levine ME, Conneely KN, Zhao H, et al. Epigenetic age acceleration, fatigue, and inflammation in patients undergoing radiation therapy for head and neck cancer: a longitudinal study. Cancer 2021;127:3361–71.
27. Dugué PA, Bassett JK, Joo JHE, Jung CH, Ming Wong E, Moreno-Betancur M, et al. DNA methylation-based biological aging and cancer risk and survival: pooled analysis of seven prospective studies. Int J Cancer 2018;142:1611–9.
28. Taylor J, Kuchel G. Bladder cancer in the elderly: clinical outcomes, basic mechanisms, and future research direction. Nat Clin Pract Urol 2009;6:135–44.
29. Molinaro AM, Lostritto K, van der Laan M. partDSA: deletion/substitution/addition algorithm for partitioning the covariate space in prediction. Bioinformatics 2010;26:1357–63.
30. Koestler DC, Marsit CJ, Christensen BC, Karagas MR, Bueno R, Sugarbaker DJ, et al. Semi-supervised recursively partitioned mixture models for identifying cancer subtypes. Bioinformatics 2010;26:2578–85.
31. Baris D, Karagas MR, Verrill C, Johnson A, Andrew AS, Marsit CJ, et al. A case-control study of smoking and bladder cancer risk: Emergent patterns over time. J Natl Cancer Inst 2009;101:1553–61.
32. Schned AR, Andrew AS, Marsit CJ, Zens MS, Kelsey KT, Karagas MR. Survival following the diagnosis of noninvasive bladder cancer: WHO/international society of urological pathology versus WHO classification systems. J Urol 2007;178:1196–200.
33. Kelsey KT, Hirao T, Schned A, Hirao S, Devi-Ashok T, Nelson HH, et al. A population-based study of immunohistochemical detection of p53 alteration in bladder cancer. Br J Cancer 2004;90:1572–6.
34. Karagas MR, Tosteson TD, Blum J, Morris JS, Baron JA, Klaue B. Design of an epidemiologic study of drinking water arsenic exposure and skin and bladder cancer risk in a U.S. population. Environ Health Perspect 1998;106:1047–50.
35. Skopp NA, Smolenski DJ, Schwesinger DA, Johnson CJ, Metzger-Abamukong MJ, Reger MA. Evaluation of a methodology to validate National Death Index retrieval results among a cohort of U.S. service members. Ann Epidemiol 2017;27:397–400.

36. Aryee MJ, Jaffe AE, Corrada-Bravo H, Ladd-Acosta C, Feinberg AP, Hansen KD, et al. Minfi: a flexible and comprehensive Bioconductor package for the analysis of Infinium DNA methylation microarrays. Bioinformatics 2014;30:1363–9.
37. Xu Z, Niu L, Li L, Taylor JA. ENmix: a novel background correction method for Illumina HumanMethylation450 BeadChip. Nucleic Acids Res 2016;44:e20.
38. Teschendorff AE, Marabita F, Lechner M, Bartlett T, Tegner J, Gomez-Cabrero D, et al. A beta-mixture quantile normalization method for correcting probe design bias in Illumina Infinium 450 k DNA methylation data. Bioinformatics 2013;29:189–96.
39. Pidsley R, Y Wong CC, Volta M, Lunnon K, Mill J, Schalkwyk LC. A data-driven approach to preprocessing Illumina 450K methylation array data. BMC Genomics 2013;14:293.
40. Johnson WE, Li C, Rabinovic A. Adjusting batch effects in microarray expression data using empirical Bayes methods. Biostatistics 2007;8:118–27.
41. Zhou W, Laird PW, Shen H. Comprehensive characterization, annotation and innovative use of Infinium DNA methylation BeadChip probes. Nucleic Acids Res 2017;45:e22.
42. Lostritto K, Strawderman RL, Molinaro AM. A partitioning deletion/substitution/addition algorithm for creating survival risk groups. Biometrics 2012;68:1146–56.
43. Christensen BC, Houseman EA, Marsit CJ, Zheng S, Wrensch MR, Wiemels JL, et al. Aging and environmental exposures alter tissue-specific DNA methylation dependent upon CPG island context. PLoS Genet 2009;5:e1000602.
44. Poage GM, Christensen BC, Houseman EA, McClean MD, Wiencke JK, Posner MR, et al. Genetic and epigenetic somatic alterations in head and neck squamous cell carcinomas are globally coordinated but not locally targeted. PLoS One 2010;5:e9651.
45. Avissar-Whiting M, Koestler DC, Houseman EA, Christensen BC, Kelsey KT, Marsit CJ. Polycomb group genes are targets of aberrant DNA methylation in renal cell carcinoma. Epigenetics 2011;6:703–9.
46. Christensen BC, Smith AA, Zheng S, Koestler DC, Houseman EA, Marsit CJ, et al. DNA methylation, isocitrate dehydrogenase mutation, and survival in glioma. J Natl Cancer Inst 2011;103:143–53.
47. Vartolomei MD, Porav-Hodade D, Ferro M, Mathieu R, Abufaraj M, Foerster B, et al. Prognostic role of pretreatment neutrophil-to-lymphocyte ratio (NLR) in patients with non–muscle-invasive bladder cancer (NMIBC): a systematic review and meta-analysis. Urol Oncol 2018;36:389–99.
48. Yıldız HA, Değer MD, Aslan G. Prognostic value of preoperative inflammation markers in non-muscle invasive bladder cancer. Int J Clin Pract 2021;75:e14118.
49. Zhang Q, Lai Q, Wang S, Meng Q, Mo Z. Clinical value of postoperative neutrophil-tolymphocyte ratio change as a detection marker of bladder cancer recurrence. Cancer Manag Res 2021;13:849–60.
50. Ferro M, Di Lorenzo G, Vartolomei MD, Bruzzese D, Cantiello F, Lucarelli G, et al. Absolute basophil count is associated with time to recurrence in patients with high-grade T1 bladder cancer receiving bacillus Calmette–Guérin after transurethral resection of the bladder tumor. World J Urol 2020;38:143–50.
51. Akan S, Ediz C, Sahin A, Tavukcu HH, Urkmez A, Horasan A, et al. Can the systemic immune inflammation index be a predictor of BCG response in patients with high-risk non-muscle invasive bladder cancer? Int J Clin Pract 2021;75:e13813.
52. Miyake M, Tatsumi Y, Gotoh D, Ohnishi S, Owari T, Iida K, et al. Regulatory T cells and tumor-associated macrophages in the tumor microenvironment in non-muscle invasive bladder cancer treated with intravesical bacille calmette-guérin: a long-term follow-up study of a Japanese cohort. Int J Mol Sci 2017;18:2186.
53. Murai R, Itoh Y, Kageyama S, Nakayama M, Ishigaki H, Teramoto K, et al. Prediction of intravesical recurrence of nonmuscle-invasive bladder cancer by evaluation of intratumoral Foxp3 + T cells in the primary transurethral resection of bladder tumor specimens. PLoS One 2018;13:e0204745.
54. Oda S, Fujisawa M, Chunning L, Ito T, Yamaguchi T, Yoshimura T, et al. Expression of Spred2 in the urothelial tumorigenesis of the urinary bladder. PLoS One 2021;16:e0254289.
55. Lv S, Wang W, Wang H, Zhu Y, Lei C. PPARγ activation serves as therapeutic strategy against bladder cancer via inhibiting PI3K-Akt signaling pathway. BMC Cancer 2019;19:204.
56. Sun M, Zhao W, Zeng Y, Zhang D, Chen Z, Liu C, et al. Fibrous sheath interacting protein 1 overexpression is associated with unfavorable prognosis in bladder cancer: a potential therapeutic target. Onco Targets Ther 2017;10:3949–56.
57. Sun M, Chen Z, Tan S, Liu C, Zhao W. Knockdown of fibrous sheath interacting protein 1 expression reduces bladder urothelial carcinoma cell proliferation and induces apoptosis via inhibition of the PI3K/AKT pathway. Onco Targets Ther 2018;11:1961–71.
58. Liu J, Yu X, Liu B, Yu H, Li Z. Phosphorylated mapk14 promotes the proliferation and migration of bladder cancer cells by maintaining runx2 protein abundance. Cancer Manag Res 2020;12:11371–82.
59. Van Puffelen JH, Novakovic B, Van Emst L, Kooper D, Zuiverloon TCM, Oldenhof UTH, et al. Intravesical BCG in patients with non-muscle invasive bladder cancer induces trained immunity and decreases respiratory infections. J Immunother Cancer 2023;11:e005518.
60. Das J, Verma D, Gustafsson M, Lerm M. Identification of DNA methylation patterns predisposing for an efficient response to BCG vaccination in healthy BCG-naïve subjects. Epigenetics 2019;14:589–601.
61. Elisia I, Lam V, Cho B, Hay M, Li MY, Kapeluto J, et al. Exploratory examination of inflammation state, immune response and blood cell composition in a human obese cohort to identify potential markers predicting cancer risk. PLoS One 2020;15:e0228633.
62. Laso FJ, Vaquero JM, Almeida J, Marcos M, Orfao A. Chronic alcohol consumption is associated with changes in the distribution, immunophenotype, and the inflammatory cytokine secretion profile of circulating dendritic cells. Alcohol Clin Exp Res 2007;31:846–54.
63. Grossmannm V, Schmitt VH, Zeller T, Panova-Noeva M, Schulz A, Laubert-Reh D, et al. Profile of the immune and inflammatory response in individuals with prediabetes and type 2 diabetes. Diabetes Care 2015;38:1356–64.